Title
S-WAVE K-N SCATTERING AMPLITUDES

Permalink
https://escholarship.org/uc/item/8xq8t06p

Authors
Kruse, Ulrich
Hauenberg, Michael.

Publication Date
1959-09-11

UCRL8888

UNIVERSITY OF
CALIFORNIA
Ernest O. Lawrence
Radiation
Laboratory

S-WAVE $\bar{K}$-N SCATTERING AMPLITUDES

UCRL-8888
Physics and Mathematics
TID-4500 (15th Ed.)

UNIVERSITY OF CALIFORNIA
Lawrence Radiation Laboratory
Berkeley, California

Contract No. W-7405-eng-48

S-WAVE $\bar{K}$-N SCATTERING AMPLITUDES

Ulrich Kruse and Michael Nauenberg

September 11, 1959

Printed for the U. S. Atomic Energy Commission

Printed in USA. Price 50 cents. Available from the
Office of Technical Services
U. S. Department of Commerce
Washington 25, D.C.

S-WAVE $\bar{K}$-N SCATTERING AMPLITUDES

Ulrich Kruse and Michael Nauenberg

Lawrence Radiation Laboratory
University of California
Berkeley, California

September 11, 1959

ABSTRACT

We describe a simple graphical method to obtain the S-Wave $\bar{K}$-N scattering amplitudes from experiment, and apply it to the most recent hydrogen bubble chamber data at 172 Mev/c K laboratory momentum. Because the cross-sections for production of neutral hyperons are still undetermined at this energy we express the results as a function of the ratios

$$r_1 = \frac{\sigma(\Sigma^0 + \lambda)}{\sigma(\Sigma^+ + \Sigma^-)} \qquad \text{and} \qquad r_2 = \frac{\sigma(\Sigma^0)}{\sigma(\Sigma^0 + \lambda)} \quad .$$

Some comments on the zero effective range approximation are also included.

S-WAVE K̄-N SCATTERING AMPLITUDES

Ulrich Kruse* and Michael Nauenberg†

Lawrence Radiation Laboratory
University of California
Berkeley, California

September 11, 1959

The S-wave K̄-N scattering amplitudes have been discussed by several authors.[1-4] Neglecting coulomb and mass-difference effects, the cross-sections $\sigma_{el.}$ and $\sigma_{c.e.}$ for K^--P elastic and charge-exchange scattering can be written in the form

$$\sigma_{el.} = \frac{\pi}{4k^2} \left| \eta_0 e^{2i\alpha_0} + \eta_1 e^{2i\alpha_1} - 2 \right|^2 \quad \ldots\ldots\ldots\ldots \quad (1)$$

and

$$\sigma_{c.e.} = \frac{\pi}{4k^2} \left| \eta_0 e^{2i\alpha_0} - \eta_1 e^{2i\alpha_1} \right|^2, \quad \ldots\ldots\ldots\ldots \quad (2)$$

where $\delta_I = \alpha_I + i\beta_I$ is the complex phase shift for isotopic spin I = 0, 1 and $\eta_I = e^{-2\beta_I}$. The absorption cross sections in I = 0 and I = 1 are given by

$$\sigma_0 = \frac{\pi}{k^2} (1 - \eta_0^2) \quad (3)$$

and

$$\sigma_1 = \frac{\pi}{k^2} (1 - \eta_1^2) \quad (4)$$

and are related to the cross sections for hyperon production by

$$\sigma_0 = 6\,\sigma\,(\Sigma^0) \quad (5)$$

and

$$\sigma_1 = 2\,\sigma\,(\Sigma^+ + \Sigma^- + \lambda) - 4\,\sigma(\Sigma^0). \quad (6)$$

---

*Permanent address: Department of Physics, University of Illinois, Urbana, Illinois.

†Summer visitor from Newman Laboratory for Nuclear Studies, Cornell University, Ithaca, New York.

We now describe a simple method to obtain the two complex phase shifts δ_0 and δ_1 from experiment. First, use Eqs. 3 to 6 to determine the quantities η_0 and η_1 from the hyperon production cross-sections. Then apply the following graphical method analogous to the technique of Ashkin and Vosko[5] to obtain α_0 and α_1 (Fig. 1.):

(a) On the complex (x, y) plane draw circles a, b, and c of radius η_0, η_1, and $\sqrt{4k^2/\pi\,\sigma_{el.}}$ centered at $A = (-2, 0)$, $B = (-2 + \sqrt{4k^2/\pi\,\sigma_{c.e.}}, 0)$ and $C = (0, 0)$, respectively.

(b) Draw the line BDE of length $2\eta_1$ through the intersection D of circles a and b in the upper half-plane.

(c) Find the intersection F of a circle of radius AE centered at A and circle c.

(d) Find the intersections G and H of a circle of radius η_1 centered at F with circle a.

It follows from the construction that the solutions are

$$\eta_0 e^{2i\alpha_0} = AH, \quad \eta_1 e^{2i\alpha_0} = HF, \quad \text{and} \quad \eta_0 e^{2i\alpha_0^{\prime}} = AG, \quad \eta_1 e^{2i\alpha_1^{\prime}} = GF$$

corresponding to the a and b solutions of Dalitz.[2] Both solutions give the same value for the elastic scattering amplitude CF. Another pair of solutions is obtained by changing the sign of α_0 and α_1, corresponding to an equivalent construction in the lower half-plane. These solutions are the (-) type solutions of Dalitz.

The elastic, charge-exchange, and charged-hyperon production $\bar{K}P$ cross sections have been measured up to 400-Mev/c K^- laboratory momentum. The neutral-hyperon production cross sections have been measured only at 300 and 400 Mev/c and at rest.[6] At 300 and 400 Mev/c, the angular distribution is no longer isotropic so that the S-wave analysis cannot be applied, and below 100 Mev/c, the coulomb and mass-difference corrections to the simple isotopic-spin formalism cannot be neglected. We have used the data at 172 Mev/c:

$$\sigma_{el.} = 79 \pm 10 \text{ mb}$$

$$\sigma_{c.e.} = 16 \pm 3 \text{ mb}$$

$$\sigma(\Sigma^+ + \Sigma^-) = 45 \pm 8 \text{ mb},$$

and obtained the solution as a function of the as yet unmeasured ratios

$$r_1 = \frac{\sigma(\Sigma^0 + \lambda)}{\sigma(\Sigma^+ + \Sigma^-)} \quad \text{and} \quad r_2 = \frac{\sigma(\Sigma^0)}{\sigma(\Sigma^0 + \lambda)} \quad . \tag{7}$$

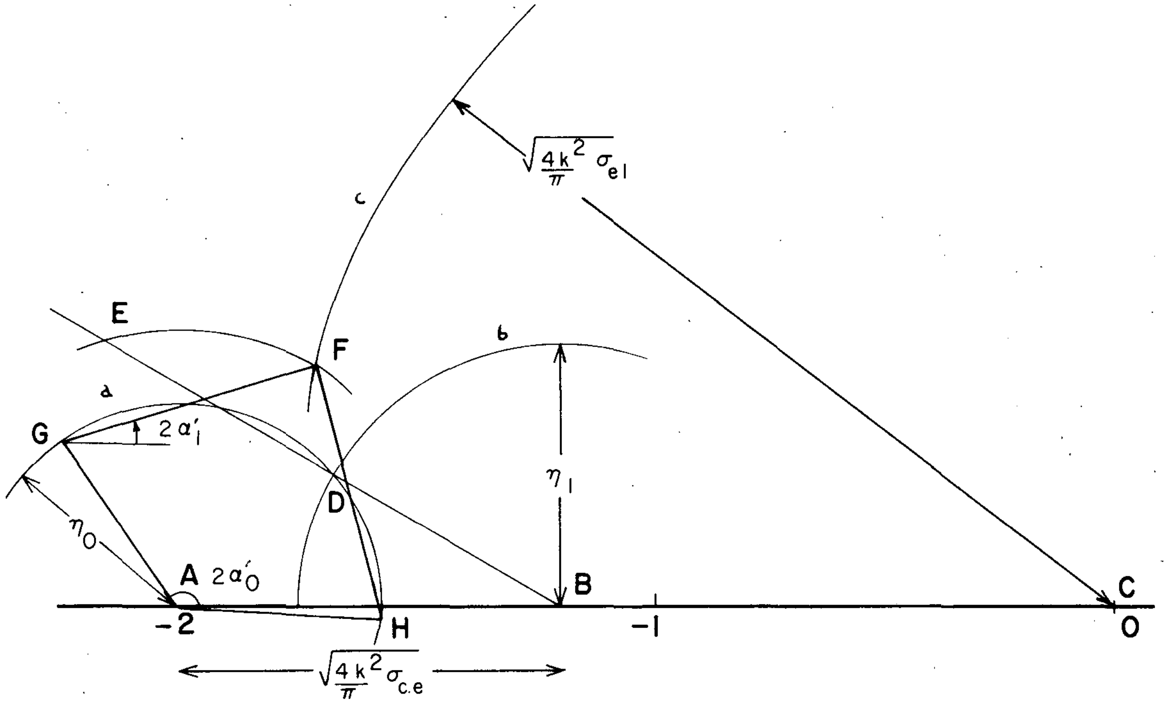

MU-18297

Fig. 1. Graphical solution for the S-wave phase shifts. (Symbols are explained in the text)

From Eqs. 3 to 6 we find

$$1 - \eta_0^2 = \frac{6k^2}{\pi} \sigma(\Sigma^+ + \Sigma^-) r_1 r_2 \tag{8}$$

and

$$1 - \eta_1^2 = \frac{2k^2}{\pi} \sigma(\Sigma^+ + \Sigma^-)[1 - (1 - 3r_2)r_1]. \tag{9}$$

In Fig. 2 we have mapped the curves of fixed η_0 and η_1 in the $(r_1 r_2)$ plane for the experimental value of $\sigma(\Sigma^+ + \Sigma^-) = 45$ mb. The physically allowed region is $0 \leqslant \eta_0^2, \eta_1^2, r_2 \leqslant 1$.

We have obtained solutions for $\eta_0 e^{2i\alpha_0}$ and $\eta_1 e^{2i\alpha_1}$ by using the mean values of the observed cross-sections and varying r_1 and r_2. An example is shown in Fig. 3. It was found that $\eta_0 e^{2i\alpha_0} + \eta_1 e^{2i\alpha_1}$ shows practically no variation with r_1 or r_2, although $\eta_0 e^{2i\alpha_0}$ and $\eta_1 {}^{2i\alpha_1}$ separately vary strongly. The graphical method has also been useful to explore the effects of uncertainties in the experimental quantities. The value of $\eta_0 e^{2i\alpha_0} + \eta_1 e^{2i\alpha_1}$ turns out to be quite insensitive to variations of $\sigma_{\text{el.}}$ and $\sigma_{\text{c.e.}}$ by a standard deviation but varies strongly when $\sigma(\Sigma^+ + \Sigma^-)$ is changed by this amount. In Fig. 4 we have plotted the points corresponding to the four assumptions about the cross sections made in Table I.

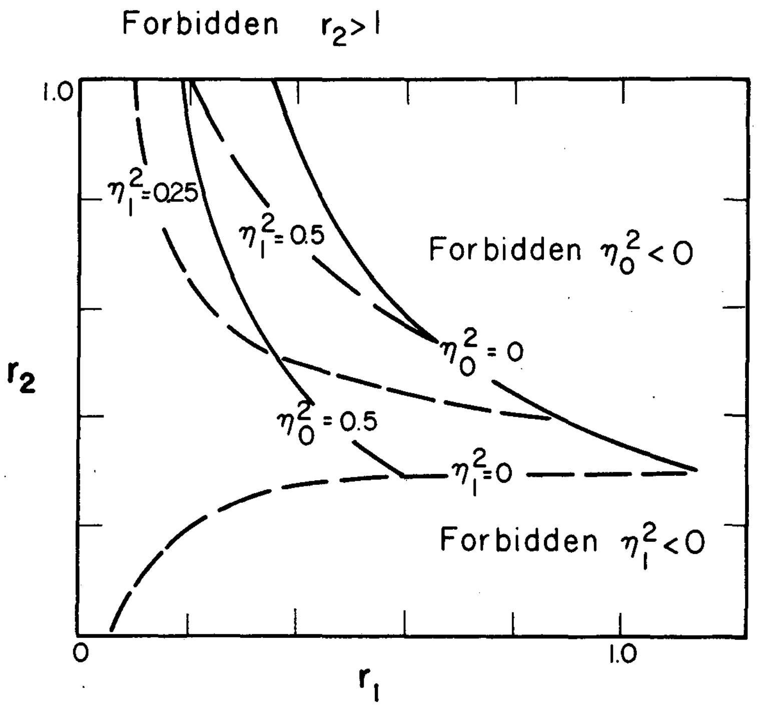

MU-18298

Fig. 2. Allowed region in the r_1, r_2 plane for $\sigma(\Sigma^+ - \Sigma^-) = 45$ mb.

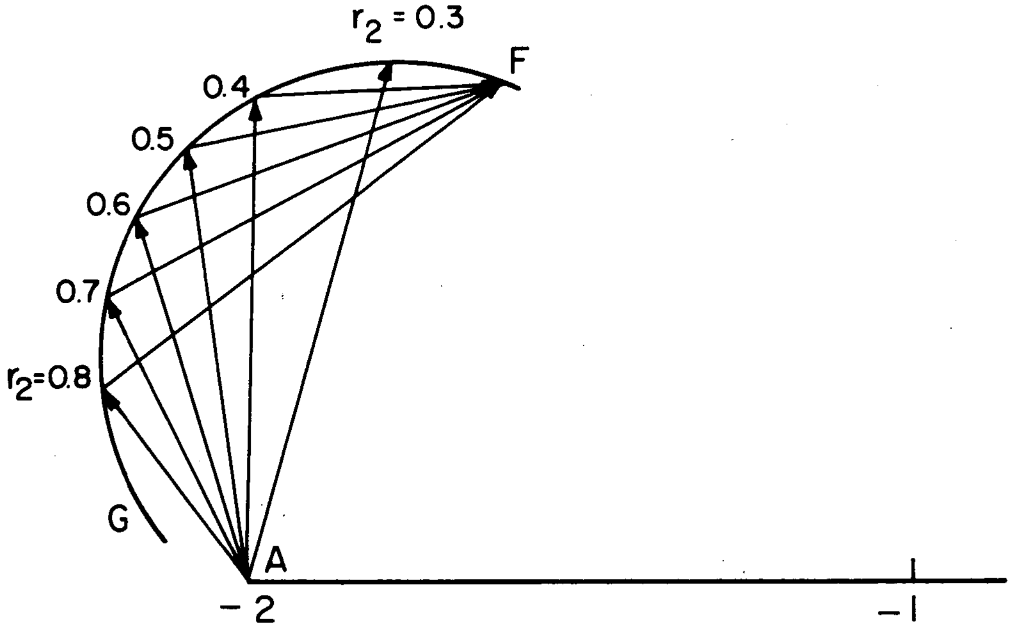

MU - 18296

Fig. 3. The vectors $AG = e^{2i\delta_0}$ and $GF = e^{2i\delta_1}$ for the b+ solution $r_1 = 0.5$, $0.3 \leqslant r_2 \leqslant 0.8$.

Table I

Assumed cross sections within standard deviation from experiment

	$\sigma_{el.}$	$\sigma_{c.e.}$	$\sigma_{\Sigma^+ + \Sigma^-}$
Exp	79 ± 10	16 ± 3	45 ± 8
F_1	79	16	45
F_2	89	16	45
F_3	79	13	45
F_4	79	16	53

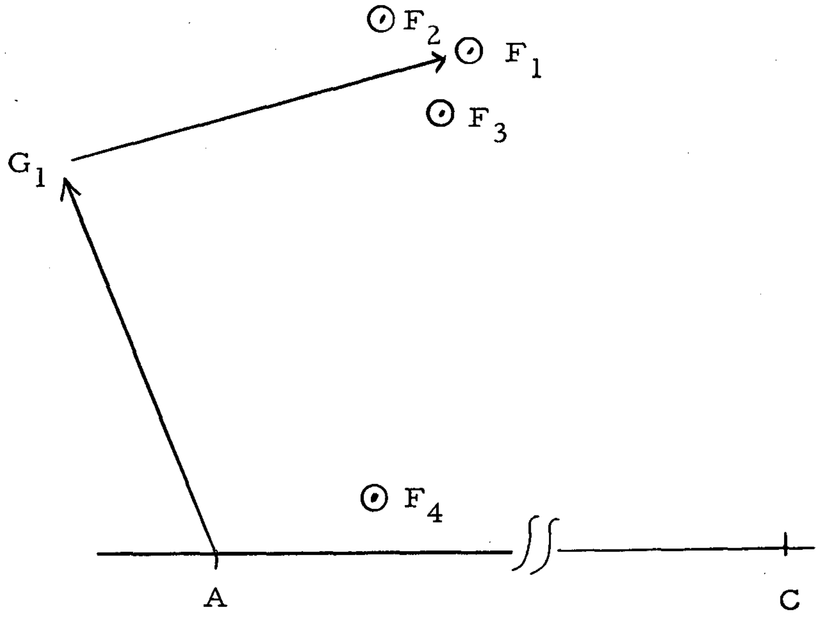

Fig. 4. Variation of $-2 + e^{2i\delta_0} + e^{2i\delta_1} = CF$ as a function of the cross sections $\sigma_{el.}$, $\sigma_{c.e.}$, and $\sigma(\Sigma^+ + \Sigma^-)$.

A zero-effective-range approximation has often been used to obtain the energy dependence of the phase shifts δ_I. In this approximation

$$kA_I = \tan \delta_I = i\left(\frac{1-\eta_I e^{2i\alpha_I}}{1+\eta_I e^{2i\alpha_I}}\right) ,$$

where $A_I = a_1 + ib_I$ is an energy-independent scattering length. In Fig. 5 we give a conformal map of the phase shifts into the A_I-complex plane. The circles correspond to the solutions obtained by making the Dalitz and Tuan assumptions concerning the neutral-hyperon production:

(a) $\sigma(\lambda) = \epsilon\sigma_1$ (ϵ = energy independent)

(b) $\frac{b_0}{b_1} = \frac{\sigma_0}{\sigma_1}$ (at rest).

Assumption (b) follows from the zero-effective-range theory in the absence of coulomb and mass differences. Jackson and Wyld have given expressions for σ_0 and σ_1 which include these effects.[3] However, there appears to be no justification in the R-matrix formalism for their method of separating the $\bar{K}P$ absorption cross section into an isotopic spin I = 0 and I = 1 part. We have not incorporated the at-rest data to restrict the solutions.

Finally, we investigated the dependence of the Dalitz-Tuan π-Y resonance[7] on r_1 and r_2. Figure 6 is a plot of the imaginary part of the $\bar{K}P$ elastic-scattering amplitude in the unphysical region for the minus solutions and various assumptions of r_1 and r_2. Note that for large r_2 the resonance disappears.

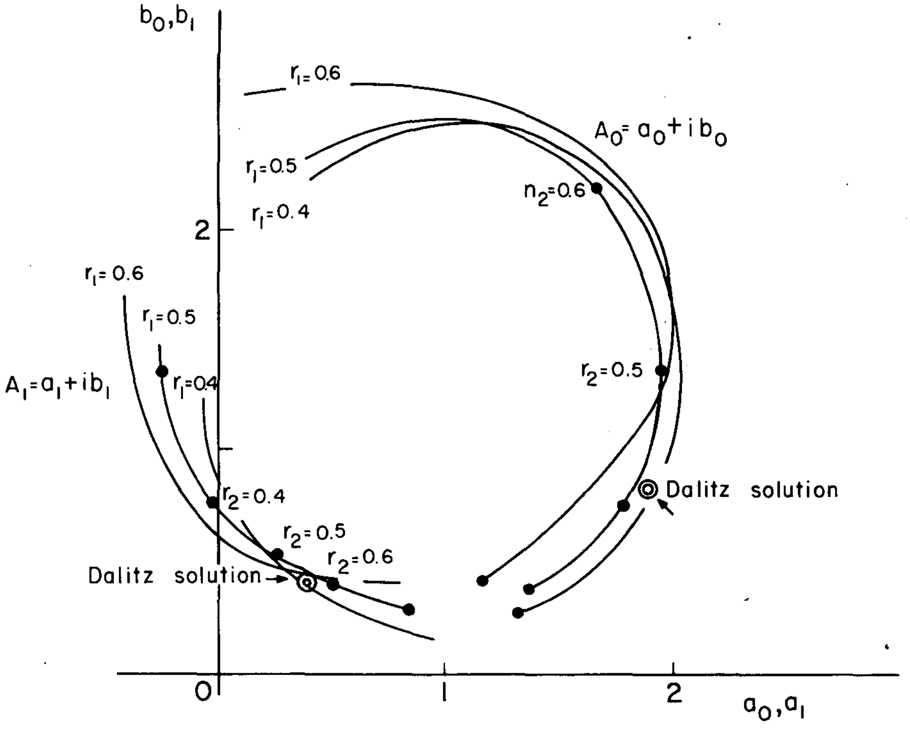

MU - 18295

Fig. 5. The complex scattering lengths $A_0 = a_0 + ib_0$ and $A_1 = a_1 + ib_1$ for $r_1 = 0.5$, $0.3 \leqslant r_2 \leqslant 0.7$. Also A_0, A_1 for the Dalitz solution with $b_0/b_1 = 2$.

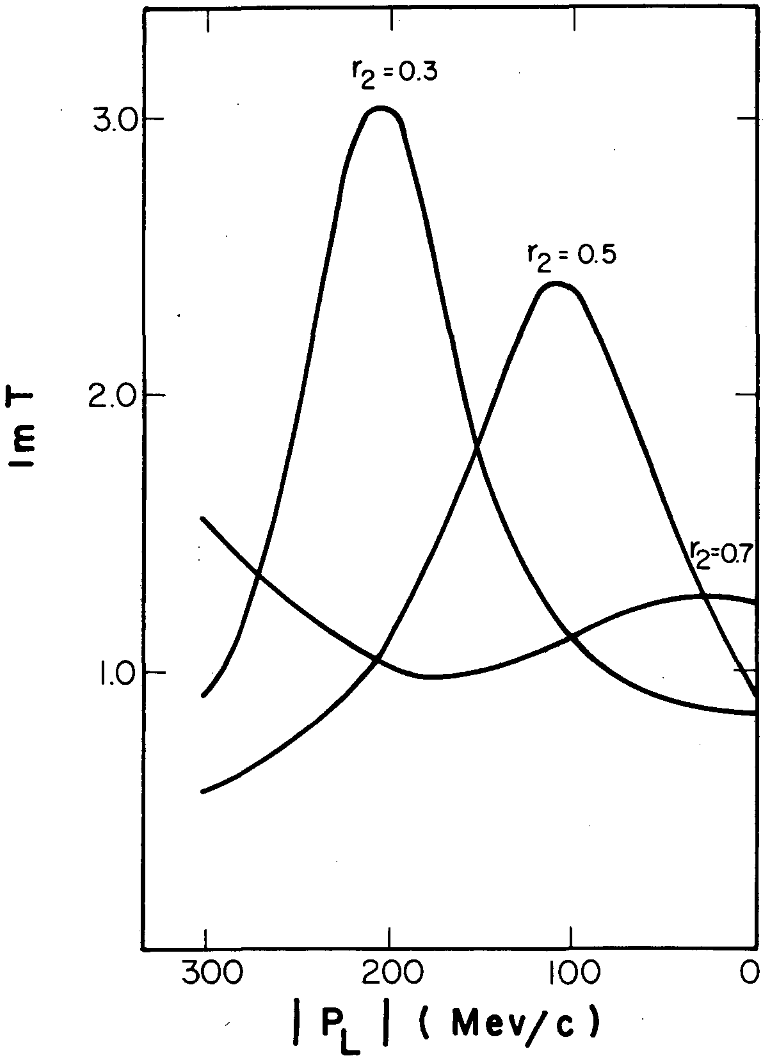

MU-18299

Fig. 6. Curves of ImT as a function of $|P_L|$ in the region of unphysical K^-P energies for the b_- solution with $r_1 = 0.5$ and $r_2 = 0.3$, 0.5, 0.7.

ACKNOWLEDGMENTS

We wish to thank Drs. Robert Tripp and Arthur Rosenfeld for discussing with us the K^-P experiments. We also gratefully acknowledge the hospitality extended to us by the Radiation Laboratory.

This work was done under the auspices of the U. S. Atomic Energy Commission.

REFERENCES

1. Jackson, Ravenhall and Wyld, Nuovo cimento 9, 834 (1958).
2. R. H. Dalitz and S. F. Tuan, The Energy Dependence of Low-Energy K^--Proton Processes, University of Chicago Report EFINS-59-17, March 1959.
3. J. D. Jackson and H. W. Wyld, Jr., Phys. Rev. Lett. 2, 355 (1959).
4. R. D. Hill, University of Illinois Technical Report No. 7 (1959).
5. J. Ashkin and S. H. Vosko, Phys. Rev. 91, 1248 (1953).
6. Robert D. Tripp, Lawrence Radiation Laboratory, private communication.
7. R. H. Dalitz and S. F. Tuan, Phys. Rev. Lett. 2, 425 (1959).

Information Division
sa